

Structural Refinements of Eulytite-Type $\text{Ca}_3\text{Bi}(\text{PO}_4)_3$ and $\text{Ba}_3\text{La}(\text{PO}_4)_3$

JACQUES BARBIER

*Department of Chemistry, McMaster University, Hamilton,
Ontario L8S 4M1, Canada*

Received February 11, 1992; in revised form April 28, 1992; accepted April 30, 1992

The room-temperature structures of the eulytite compounds $\text{Ca}_3\text{Bi}(\text{PO}_4)_3$ and $\text{Ba}_3\text{La}(\text{PO}_4)_3$ have been refined using powder neutron diffraction data. The metal atoms are disordered on a single site of the $I\bar{4}3d$ space group, whereas the oxygen atoms are split between two sites, giving rise to rotational disorder of the phosphate anion similar to that previously observed in $\text{Sr}_3\text{La}(\text{PO}_4)_3$. The degree of oxygen disorder depends on the nature of the metal atoms and, in particular, is reduced when Bi^{3+} ions are present in the eulytite structure. © 1992 Academic Press, Inc.

1. Introduction

Until recently, the only representatives of the eulytite structure type to have been characterized in detail were the bismuth silicate and germanate, $\text{Bi}_4(\text{XO}_4)_3$ ($X = \text{Si}, \text{Ge}$), the structures of which have been determined by single crystal X-ray and neutron diffraction (1–5). Both compounds are completely isostructural with each other, containing only slightly distorted XO_4 tetrahedra and the expected distorted octahedral coordination around the lone-pair Bi^{3+} ions. Numerous double phosphates of the type $\text{A}_3\text{B}(\text{PO}_4)_3$ ($A =$ alkaline earth or Pb; $B =$ trivalent rare earth, Y, In, or Bi) also adopt the eulytite structure (6–10) and, based on X-ray powder data, they have usually been assumed to be simply isostructural with $\text{Bi}_4(\text{SiO}_4)_3$. However, the first structural refinement of a eulytite-type phosphate, namely $\text{Sr}_3\text{La}(\text{PO}_4)_3$, recently carried out using powder neutron diffraction (11), has revealed the presence of significant positional disorder on the oxygen sublattice, the

origin of which could be linked to the bonding requirements of the metal atoms. In order to obtain further insights into the crystal chemistry of phosphate eulytites and, in particular, to study the dependence of the structural disorder on the nature of the metal atoms, the structures of the two compounds, $\text{Ca}_3\text{Bi}(\text{PO}_4)_3$ and $\text{Ba}_3\text{La}(\text{PO}_4)_3$, have been refined using powder neutron data. The results of these refinements are the subject of the present paper.

2. Experimental

Powder samples of approximately 8 g were prepared from stoichiometric mixtures of $(\text{CaCO}_3 + \text{Bi}_2\text{O}_3 + \text{NH}_4\text{H}_2\text{PO}_4)$ and $(\text{Ba}(\text{HCOO})_2 + \text{La}_2\text{O}_3 + \text{NH}_4\text{H}_2\text{PO}_4)$ powders, respectively. After a first firing at 500–600°C for decomposing the carbonate, oxalate, and ammonium phosphate, the eulytite phases were synthesized at 850°C in the case of $\text{Ca}_3\text{Bi}(\text{PO}_4)_3$ and in the range 1200–1400°C in the case of $\text{Ba}_3\text{La}(\text{PO}_4)_3$. The single-phase nature of the final products

TABLE I
UNIT-CELL PARAMETERS OF SOME EULYTITE
COMPOUNDS REFINED USING POWDER X-RAY DATA

Compound	a (Å)	Reference
Ba ₃ La(PO ₄) ₃	10.5241(5)	7, this work
Ca ₃ Bi(PO ₄) ₃	9.9772(4)	7, this work
Ca ₃ La(PO ₄) ₃	9.9400(7)	9, this work
Ca ₃ Y(PO ₄) ₃	9.835	10
Ca ₃ Yb(PO ₄) ₃	9.8199(4)	This work

was checked by powder X-ray diffraction using a Guinier–Hägg camera. The powder patterns could be entirely indexed on cubic eulytite-type unit cells in the $\bar{I}43d$ space group, with cell parameters in good agreement with previous reports (7–9). The cell dimensions of Ca₃Bi(PO₄)₃ and Ba₃La(PO₄)₃ are listed in Table I together with those of several other Ca-based phosphate eulytites. It is worth pointing out that Ca₃Bi(PO₄)₃ is apparently the only Ca eulytite that can be synthesized at moderate temperature, whereas all the others decompose below about 1200°C (9, 10).

The neutron powder diffraction data were collected at the McMaster Nuclear Reactor using 1.3907-Å neutrons obtained from a [200] copper monochromator with the samples contained in thin-walled vanadium cans. The diffraction patterns were recorded at four different settings of the position-sensitive detector over the angular range 15°–90° (2θ). After correction of the raw data for detector geometry (12), profile refinements were carried out with a local version of the Rietveld program. The following scattering lengths (10^{-12} cm) were used in the refinements: 0.490 (Ca), 0.853 (Bi),

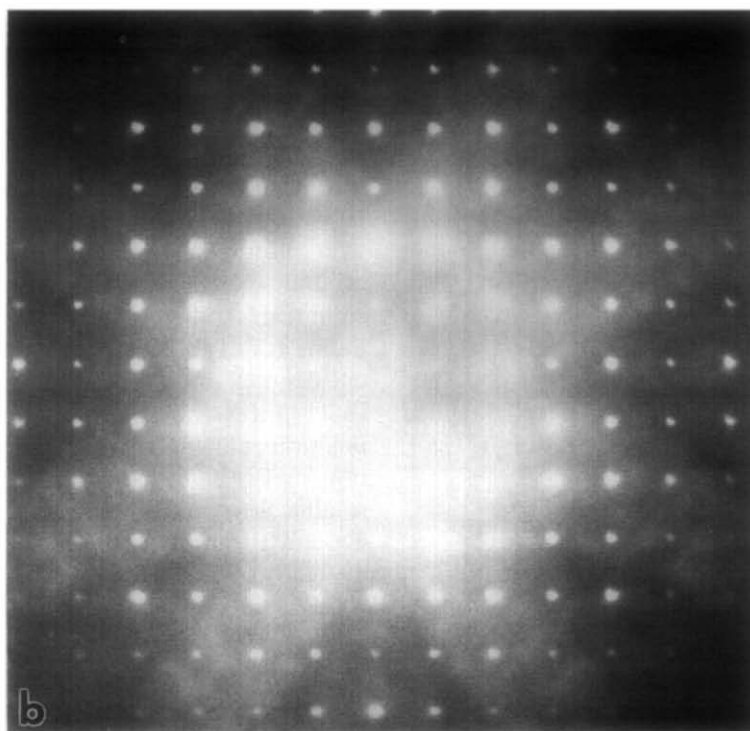
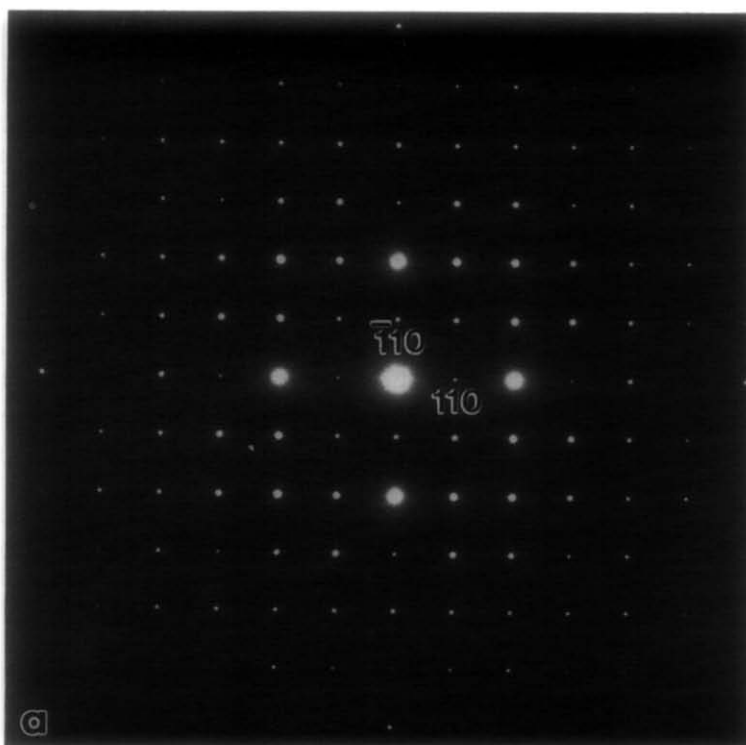
0.525 (Ba), 0.824 (La), 0.513 (P), and 0.581 (O) (13).

3. Structure Refinements

An initial attempt was made to refine the Ca₃Bi(PO₄)₃ structure using the atomic positions determined previously for the fully ordered eulytite, Bi₄(SiO₄)₃ (2, 3, 11). This model, however, resulted in poor agreement indices (nuclear $R_n = 13.1\%$ and weighted profile $R_{wp} = 8.6\%$) as well as a high isotropic temperature factor for the unique oxygen atom ($B = 4.1 \text{ \AA}^2$). This result was taken as an indication of oxygen disorder which was also suggested by the relatively high background in the neutron powder pattern. As shown in Fig. 1, electron diffraction patterns of Ca₃Bi(PO₄)₃ also contained a strong, diffuse background which was completely absent in the case of Bi₄(SiO₄)₃.

Accordingly, the refinement of the Ca₃Bi(PO₄)₃ structure was restarted using the atomic positions obtained earlier for the disordered Sr₃La(PO₄)₃ phase (10); the Ca and Bi atoms were randomly distributed on the 16c sites of the $\bar{I}43d$ space group, the P atoms were fixed on the 12a sites, and the O atoms were uniformly distributed over three equivalent 48e sites, each one-third occupied. The structural parameters allowed to vary during the refinement included the cell dimension, the atomic positions, the isotropic temperature factors (one B parameter for all oxygens), and the populations of the three oxygen sites. During the refinement, the population of one oxygen site dropped steadily to very low values with large e.s.d.'s for the corresponding coordinates. Therefore, a new refinement using

FIG. 1. [001] electron diffraction patterns of Bi₄(SiO₄)₃ (a) and Ca₃Bi(PO₄)₃ (b). In both cases, the {200} and {110} reflections (forbidden in the $\bar{I}43d$ space group) appear by double diffraction (e.g., (200) = (130) + ($\bar{1}30$) and (110) = (400) + ($\bar{3}10$)). The {100} reflections (also forbidden) are absent. Note the pronounced diffuse background in the pattern of Ca₃Bi(PO₄)₃.



two oxygen sites only was carried out which eventually converged to an agreement index $R_{wp} = 5.7\%$. The observed and calculated diffraction profiles are shown in Fig. 2a and the final structural parameters together with details of the refinement are listed in Table II.

The powder neutron diffraction pattern of $\text{Ba}_3\text{La}(\text{PO}_4)_3$ showed a higher and more irregular background than that of $\text{Ca}_3\text{Bi}(\text{PO}_4)_3$, indicating a higher degree of structural disorder. Nevertheless, for the purpose of comparison, the same model based on two partially occupied oxygen sites was used to refine the $\text{Ba}_3\text{La}(\text{PO}_4)_3$ structure. Following the same procedure as that for the Ca eulytite, the refinement converged to an agreement index $R_{wp} = 5.3\%$ only, however, after removing parts of the data which were particularly strongly affected by the background ($31^\circ < 2\theta < 35^\circ$ and $2\theta > 75^\circ$). Although the exact origin of the background jump or hump near $2\theta = 33^\circ$ is not known, it possibly corresponds to scattering from poorly crystallized products from the incipient decomposition of the eulytite phase during quenching. The observed and calculated diffraction profiles are shown in Fig. 2b and the final structural parameters with details of the refinement are listed in Table II. It should be noted that the much higher oxygen temperature factor in $\text{Ba}_3\text{La}(\text{PO}_4)_3$ (4.6 \AA^2 as compared to 1.8 \AA^2 in $\text{Ca}_3\text{Bi}(\text{PO}_4)_3$) reflects a greater oxygen disorder, probably similar to that observed in $\text{Sr}_3\text{La}(\text{PO}_4)_3$ which has been modeled using three different oxygen sites (11).

4. Description of the Crystal Structures

The structural arrangements in $\text{Ca}_3\text{Bi}(\text{PO}_4)_3$, $\text{Ba}_3\text{La}(\text{PO}_4)_3$, and, for comparison, $\text{Bi}_4(\text{SiO}_4)_3$ are shown in Fig. 3 projected along the [001] direction of the eulytite unit cell. As described previously (11), the eulytite structure can be viewed as a packing

of face-sharing, twisted M_8 bisdisphenoids ($M = \text{metal atom}$) centered by quasi-regular PO_4 (SiO_4) tetrahedra. In $\text{Bi}_4(\text{SiO}_4)_3$, the unique oxygen position leads to a well-defined, parallel orientation of the SiO_4 tetrahedron and the Bi_8 bisdisphenoid, the oxygen atoms being 3-coordinated ($2\text{Bi} + \text{Si}$) and the Bi atoms having the expected, distorted ($3 + 3$) octahedral coordination. The structural disorder present in the $\text{Ca}_3\text{Bi}(\text{PO}_4)_3$ and $\text{Ba}_3\text{La}(\text{PO}_4)_3$ eulytites corresponds to a clockwise or anticlockwise rotation of the PO_4 tetrahedron around its $\bar{4}$ axis, so that the oxygen atoms move toward the centers of $M_3\text{P}$ tetrahedra and become 4-coordinated. At the same time, it follows that the coordination of the metal atoms increases from 6 ($3 + 3$) to 9 ($3 + 3 + 3$) (note that the M atoms are located on the threefold axes of the cubic unit cell). This rotational disorder of the phosphate group is identical to what has been found in the case of $\text{Sr}_3\text{La}(\text{PO}_4)_3$ (11).

The bond lengths and angles listed in Table III show that, in both the $\text{Ca}_3\text{Bi}(\text{PO}_4)_3$ and the $\text{Ba}_3\text{La}(\text{PO}_4)_3$ structures, the phosphate group remains quite regular with normal P–O bond lengths and angular distortions similar to those observed for the tetrahedral groups in $\text{Bi}_4(\text{SiO}_4)_3$ and $\text{Bi}_4(\text{GeO}_4)_3$ (4, 5). The two structures, however, differ markedly in the coordinations around the metal atoms as a result of significant shifts in the positions of the M atoms (cf. Table II) combined with different degrees of oxygen disorder (cf. Fig. 3). In $\text{Ca}_3\text{Bi}(\text{PO}_4)_3$, the more populated O(1) position remains close to the oxygen position in $\text{Bi}_4(\text{SiO}_4)_3$ and, thus, the structure retains a sixfold coordination around the Ca and Bi atoms with an average $M\text{--O}(1)$ distance of 2.36 \AA , close to the expected Ca–O and Bi–O bond lengths (2.38 and 2.41 \AA , respectively (14)). The O(2) position yields a rather irregular ninefold coordination around the metal atoms with a much larger average $M\text{--O}(2)$ distance of

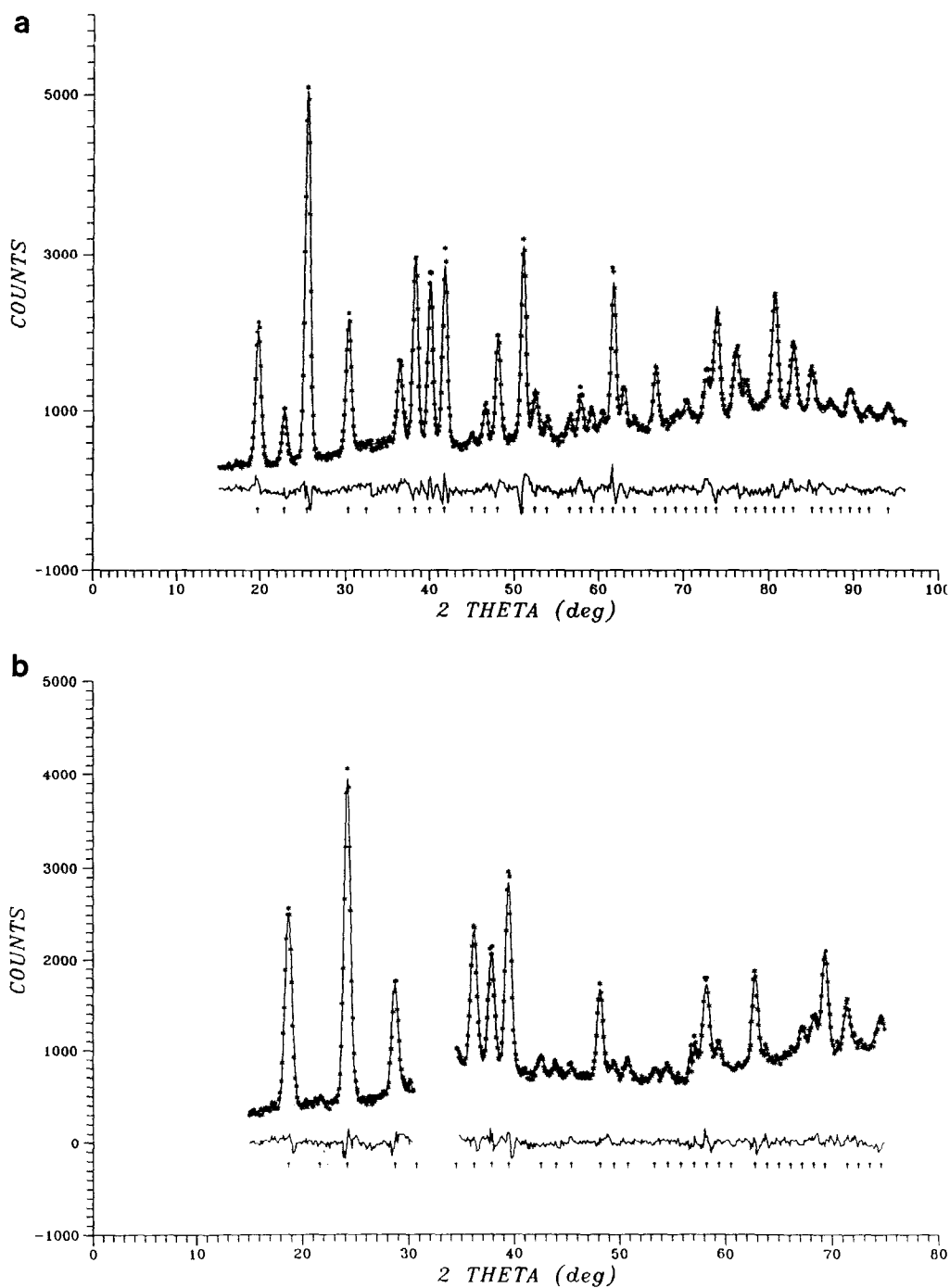


FIG. 2. Observed (+) and calculated (full line) powder neutron diffraction profiles for $\text{Ca}_3\text{Bi}(\text{PO}_4)_3$ (a) and $\text{Ba}_3\text{La}(\text{PO}_4)_3$ (b). The arrows indicate the Bragg peak positions. Some data had to be eliminated from the $\text{Ba}_3\text{La}(\text{PO}_4)_3$ pattern because of strong variations in the background.

TABLE II
RESULTS OF THE STRUCTURAL REFINEMENTS OF THE EULYTITE PHASES $\text{Ca}_3\text{Bi}(\text{PO}_4)_3$ AND $\text{Ba}_3\text{La}(\text{PO}_4)_3$ IN THE $I\bar{4}3d$ SPACE GROUP, USING A SINGLE METAL SITE AND TWO PARTIALLY OCCUPIED OXYGEN SITES

			$\text{Ca}_3\text{Bi}(\text{PO}_4)_3$	$\text{Ba}_3\text{La}(\text{PO}_4)_3$
<i>M</i>	16 <i>c</i>	<i>x</i>	0.0729(3)	0.0602(5)
		<i>B</i> (Å ²)	1.9(2)	1.6(2)
P	12 <i>a</i>	<i>B</i> (Å ²)	1.4(2)	1.0(2)
O(1)	48 <i>e</i>	<i>x</i>	0.5242(9)	0.4663(17)
		<i>y</i>	0.3768(5)	0.3614(11)
		<i>z</i>	0.7094(5)	0.7075(16)
		<i>B</i> (Å ²)	1.8(1)	4.6(3)
		Pop	30.0(6)	17.0(4)
O(2)	48 <i>e</i>	<i>x</i>	0.5860(15)	0.5733(12)
		<i>y</i>	0.3422(8)	0.3432(5)
		<i>z</i>	0.7062(9)	0.7021(8)
		<i>B</i> (Å ²)	B[O(1)]	B[O(1)]
		Pop	48-pop[O(1)]	48-pop[O(1)]
Agreement indices		<i>R</i> _{wp}	0.057	0.053
		<i>R</i> _n	0.057	0.060
		<i>R</i> _c	0.027	0.029
No. data points			815	563
No. frames with linear background			5	3
No. variables			27	23
Line shape			Gaussian	Gaussian
Half-width parameters ($\times 10^4$)		<i>U</i>	1.7(2)	1.8(3)
		<i>V</i>	-1.5(2)	-1.6(3)
		<i>W</i>	0.78(3)	0.78(4)

Note. Numbers in parentheses represent e.s.d.'s on the last significant digit.

2.64 Å. But it should be noted that both the O(1) and the O(2) oxygen positions yield one set of short *M*-O distances (2.28 and 2.36 Å, respectively) which appear to be required by the presence of lone-pair Bi^{3+} ions on the metal sites. Indeed, the $\text{Bi}_4(\text{SiO}_4)_3$ and $\text{Bi}_4(\text{GeO}_4)_3$ eulytites contain even shorter Bi-O bonds (2.16 Å) with an average Bi-O bond length of approximately 2.38 Å (3, 5, 11). No such requirement for short bonds exists in the $\text{Ba}_3\text{La}(\text{PO}_4)_3$ structure and, accordingly, the O(1) and O(2) positions are further apart, both leading to a more regular ninefold coordination around the larger metal atoms. The mean *M*-O(1) (2.84 Å) and *M*-O(2) (2.80 Å) bond lengths in $\text{Ba}_3\text{La}(\text{PO}_4)_3$ are also in good agreement with

the expected weighted bond distance (2.76 Å for *M* = 3Ba + La (14)).

5. Discussion

The present refinements of the $\text{Ca}_3\text{Bi}(\text{PO}_4)_3$ and $\text{Ba}_3\text{La}(\text{PO}_4)_3$ structures confirm that the detailed atomic arrangement of the eulytite structure type depends on the nature of the metal atoms. Disorder on the oxygen sublattice of the type described here, i.e., rotational disorder of the tetrahedral group, can be expected to occur in all mixed metal eulytites which, in fact, represent all known compounds with the exception of $\text{Bi}_4(\text{XO}_4)_3$ (*X* = Si, Ge). This intrinsic structural disorder is associated with the different metal-oxygen bond lengths and its

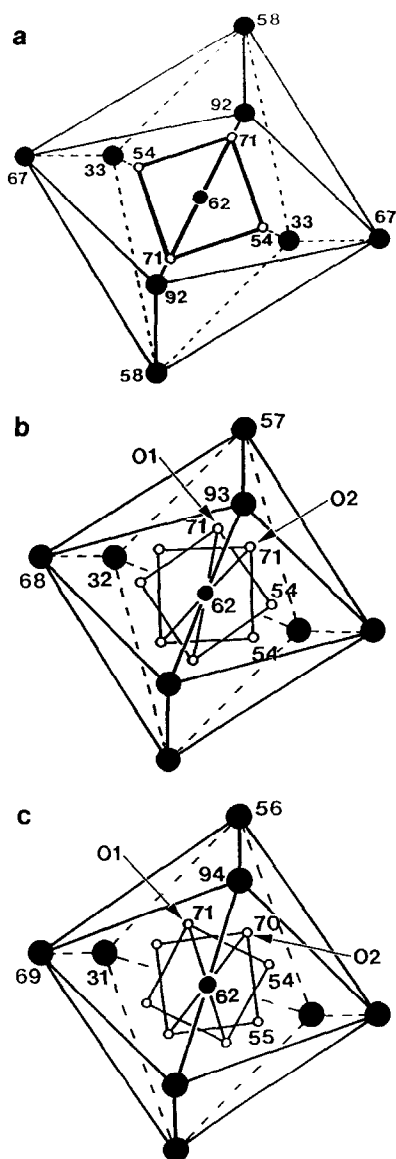


FIG. 3. Part of the eulytite structure viewed along the [001] direction for $\text{Bi}_4(\text{SiO}_4)_3$ (a), $\text{Ca}_3\text{Bi}(\text{PO}_4)_3$ (b), and $\text{Ba}_3\text{La}(\text{PO}_4)_3$ (c). Large, medium, and small circles represent metal, phosphorus (or silicon), and oxygen atoms, respectively. Atom heights are given in units of $a/100$. In the phosphate eulytites, the oxygen atoms are split between two positions, giving rise to rotational disorder of the PO_4 tetrahedra.

presence suggests that most eulytite phases may be thermodynamically stable at high temperature only. This is certainly the case for the Ca-based eulytites, $\text{Ca}_3\text{Ln}(\text{PO}_4)_3$ ($\text{Ln} = \text{Y}$, rare earth) (9, 10) and probably also for eulytites such as $\text{Ba}_3\text{Yb}(\text{PO}_4)_3$ in which the size mismatch between the metal atoms is large (11). As well as being unstable at room temperature, the calcium eulytites seem also to be the most disordered: an attempt at refining the $\text{Ca}_3\text{La}(\text{PO}_4)_3$ structure as part of the present study proved unsuccessful due to the very irregular background in the neutron powder pattern. Electron diffraction patterns also contained strong, diffuse background features and lattice images showed random contrast variations which could be associated with disorder on a unit-cell scale.

As already noted by previous authors (6, 7) and as shown by the formation of $\text{Ca}_3\text{Bi}(\text{PO}_4)_3$ at 850°C , the presence of lone-pair Bi^{3+} ions stabilizes the eulytite structure at lower temperature. The present study shows further that it also reduces the degree of structural disorder by retaining the oxygen atoms in positions close to that observed in $\text{Bi}_4(\text{SiO}_4)_3$ or $\text{Bi}_4(\text{GeO}_4)_3$. Thus, the degree of disorder should decrease with increasing Bi content and this could be shown by, for

TABLE III
SELECTED BOND LENGTHS (Å) AND ANGLES (DEGREES) IN $\text{Ca}_3\text{Bi}(\text{PO}_4)_3$ AND $\text{Ba}_3\text{La}(\text{PO}_4)_3$

	$\text{Ca}_3\text{Bi}(\text{PO}_4)_3$	$\text{Ba}_3\text{La}(\text{PO}_4)_3$
$M-\text{O}(1)$	$2.280(7) \times 3$	$2.764(18) \times 3$
	$2.431(7) \times 3$	$2.786(16) \times 3$
	$[3.517(9) \times 3]$	$2.966(18) \times 3$
$M-\text{O}(2)$	$2.363(11) \times 3$	$2.705(12) \times 3$
	$2.660(11) \times 3$	$2.732(10) \times 3$
	$2.894(14) \times 3$	$2.974(13) \times 3$
$\text{P}-\text{O}(1)$	$1.538(5) \times 4$	$1.502(14) \times 4$
$\text{P}-\text{O}(2)$	$1.495(11) \times 4$	$1.488(9) \times 4$
$\text{O}(1)-\text{P}-\text{O}(1)$	107.4–113.6	109.3–109.5
$\text{O}(2)-\text{P}-\text{O}(2)$	107.0–114.4	107.3–114.0

instance, investigating solid solutions of the type $M_x\text{Bi}_{4-x}(\text{SiO}_4)_3$ (M = trivalent yttrium or rare earth). Apart from Bi, other large atoms such as Ba or Pb also appear to have a stabilizing effect on the eulytite structure: for example, the compounds $\text{Ba}_3\text{La}(\text{PO}_4)_3$ and $\text{Pb}_3\text{La}(\text{PO}_4)_3$ are readily synthesized at temperatures around 1100°C (e.g., 6, 7), whereas the Ca analog can be obtained only as a single phase by quenching from 1300 to 1400°C (9, 11). It would therefore be of interest to carry out structure refinements of eulytite phases containing only Ba or Pb metal atoms and determine the degree of disorder on their oxygen sublattice. In such phases, the metal atoms are likely to be 9-coordinated and the oxygen atoms may thus be forced into positions close to either the O(1) or the O(2) site of the $\text{Ba}_3\text{La}(\text{PO}_4)_3$ structure (cf. Fig. 3). However, the only Ba- or Pb-based eulytites known to date are mixed phases such as $\text{Ba}_4(\text{PO}_4)_2\text{SO}_4$ (6), $\text{Pb}_4(\text{PO}_4)_2\text{SO}_4$, and $\text{Pb}_4(\text{PO}_4)_2\text{CrO}_4$ (15), for which the small size difference between the tetrahedral groups may be an additional source of disorder. Their structural investigation by powder neutron diffraction is now in progress.

Acknowledgment

This work was supported by an operating grant from the Natural Sciences and Engineering Research Council of Canada.

References

1. G. MENZER, *Z. Kristallogr.* **78**, 136 (1931).
2. D. J. SEGAL, R. P. SANTORO, AND R. E. NEWNHAM, *Z. Kristallogr.* **123**, 73 (1966).
3. J. LEWIS, Dissertation, Technische Universität Clausthal (1978).
4. P. FISHER AND F. WALDNER, *Solid State Commun.* **44**, 657 (1982).
5. S. F. RADAEV, L. A. MURADYAN, YU F. KARGIN, V. A. SARLIN, V. N. KANEPIT, AND V. I. SIMONOV, *Sov. Phys. Crystallogr.* **35**, 204 (1990).
6. G. BLASSE, *J. Solid State Chem.* **2**, 27 (1970).
7. G. ENGEL, *Z. Anorg. Allg. Chem.* **387**, 22 (1972).
8. G. ENGEL AND W. KIRCHBERGER, *Z. Anorg. Allg. Chem.* **417**, 81 (1975).
9. G. J. MCCARTHY AND D. E. PFOERTSCH, *J. Solid State Chem.* **38**, 128 (1981).
10. W. SZUSZKIEWICZ AND T. ZNAMIEROWSKA, *J. Solid State Chem.* **88**, 406 (1990).
11. J. BARBIER, J. E. GREEDAN, T. ASARO, AND G. J. MCCARTHY, *Eur. J. Solid State Inorg. Chem.* **27**, 855 (1990).
12. C. W. TOMPSON, D. F. R. MILDNER, M. MEHDREGANG, J. SUDOL, R. BERLINER, AND W. B. YELON, *J. Appl. Crystallogr.* **17**, 385 (1984).
13. V. F. SEARS, in "Methods of Experimental Physics" (K. Sköld and D. L. Price, Eds.), Vol. 23, Part A, Academic Press, San Diego (1986).
14. R. D. SHANNON, *Acta Crystallogr. A* **32**, 751 (1976).
15. A. DURIF-VARAMBON, *Bull. Soc. Fr. Miner. Crist.* **82**, 285 (1959).